A. Carnicero
Tenured Assistant Professor
e-mail: carnicero@upcomillas.es

J. R. Jimenez-Octavio
Assistant Professor

C. Sanchez-Rebollo
Doctoral Fellow

Institute for Research in Technology,
ETSI-ICAI,
Universidad Pontificia Comillas,
28015 Madrid, Spain

A. Ramos
Product Engineer
Fuel Rod Technology Engineering,
ENUSA,
28040 Madrid, Spain

M. Such
Structures Engineer
Mechanical Department,
ESTEC,
European Space Agency,
2200 AG Noordwijk, The Netherlands

Influence of Track Irregularities in the Catenary-Pantograph Dynamic Interaction

This paper presents an advanced pantograph-catenary-vehicle-track model, which allows us to analyze the vertical dynamics of the complete system. The developed model is able to evaluate the displacements and the contact force generated in the catenary-pantograph as well as the wheel-track interactions. Nevertheless, this paper focuses on the possible influence of track irregularities on the catenary-pantograph dynamic interaction. From a power spectral density function of the track irregularities, 180 track profiles and their respective catenary-pantograph-vehicle-track simulations have been generated. The wide range of results allows us to obtain some conclusions about the influence of the track profile in the catenary-pantograph behavior. [DOI: 10.1115/1.4006735]

1 Introduction

In railway systems, the catenary-pantograph interaction is the phenomenon responsible for the transmission and the raising of the electric energy from the power supply to the locomotive. The quality of this raising, the circulation speed, and the maintainability of the infrastructure depend on the design and the running of this system. There are many analyses of the dynamic behavior of the catenary-pantograph system, so it is worthy to mention the surveys related to this topic developed by Poetsch et al. in Ref. [1] and Shabana and San in Ref. [2], the simulation of the catenary-pantograph dynamics using the finite element method (FEM) presented in Ref. [3] by Collina and Bruni, the simplified models developed in Ref. [4] by Wu and Brennan and improved in Ref. [5] by Lopez-Garcia et al., or the mathematical model of Arnold and Simeon presented in Ref. [6].

As far as the drive system of the majority of the trains is based on the wheel-track contact, the study of the global dynamic of this system is known as vehicle-track interaction. Obviously, the quality of this contact affects the passenger comfort, the noise emission, and the maintainability of the set, among others. There exist many studies about the global dynamics of the vehicle-track set: on the one hand by using moving loads and moving elements in both Refs. [7] and [8] developed by Olsson and Koh et al. respectively and, on the other hand, by using an analysis of this interaction and its influence on traffic when trains pass over bridges presented by Lou in Refs. [9] and [10]. In Ref. [11], Zhai et al. present a full 3D vehicle-track model, which allows us to consider not only the vertical dynamics, considering the vertical rail irregularities, but also the transversal movements, taking into account the rail alignment irregularities too. Likewise, Pombo et al. provide a detailed description of the wheel-track contact in Ref. [12]. These same authors publish in Ref. [13] another work related to the previous one, but considering the effect of irregularities along the track in order to quantify the influence of this phenomenon on the wear of the rails. Seo et al. formulate in Ref. [14] a full theoretical 3D catenary-pantograph-vehicle-track model based on multibody dynamics techniques. However, the results presented are uniquely referred to the catenary-pantograph interaction without considering its coupling with the vehicle and the track. The work of Zhai and Cai [15] is worth mentioning in this particular issue. This paper presents the influence of the vehicle system vibrations induced by the irregularities of track on the catenary-pantograph interaction. This work is based on independent models for the two subsystems: vehicle-track and catenary-pantograph. Thus, the displacements obtained within the first subsystem are imposed on the second one. Due to the notable number of simulations carried out in the paper presented herein and the statistical analysis of the obtained results, it could be considered that its contribution expands the conclusions summarized by Zhai and Cai. In addition, the results presented in this paper have been obtained along a high speed catenary, unlike the results published in Ref. [15] by Zhai and Cai, which are referred to as a conventional catenary.

Apart from this introduction, the present paper has been organized according to its main purpose: to analyze the influence of the track irregularities in the catenary-pantograph dynamic interaction. Thus, the paper is structured as follows: a description of the interaction subsystems catenary-pantograph and vehicle-track together with their validations are presented in Secs. 2 and 3, respectively, a description of the coupling of the whole system catenary-pantograph-vehicle-track is presented in Sec. 4, the results intended within this work are shown and detailed in Sec. 5, and, finally, concluding remarks are given in Sec. 6.

Contributed by the Design Engineering Division for publication in the JOURNAL OF COMPUTATIONAL AND NONLINEAR DYNAMIC. Manuscript received November 24, 2011; final manuscript received April 12, 2012; published online July 20, 2012. Assoc. Editor: Tae-Won Park.

2 Catenary-Pantograph Model

The catenary model applied in this work is based on a nonlinear finite elements' discretization of the geometry of the

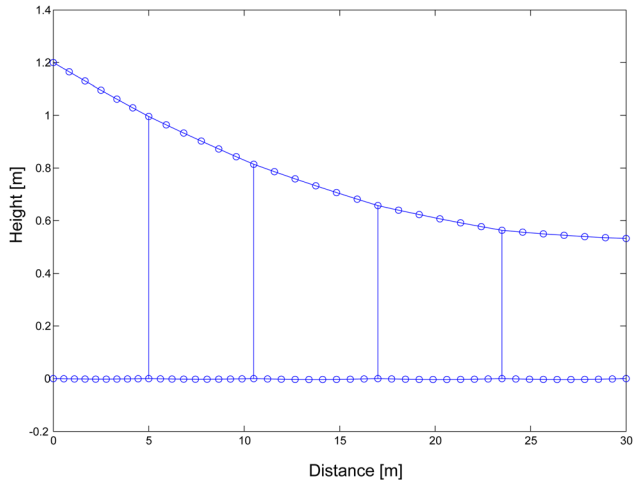

Fig. 1 Catenary model

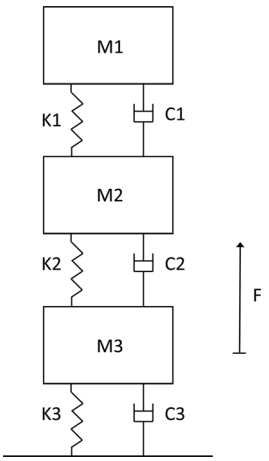

Fig. 2 Three degrees of freedom pantograph model

Table 1 Simulation values of DSA-380E pantograph

	1	2	3
M (kg)	6.6	5.8	5.8
C (Ns/m)	70	70	70
K (N/m)	9.4×10^3	14.1×10^3	0.08

Table 2 Validation of the catenary-pantograph model at 250 km/h

Magnitude	Range	Model
Mean contact force (N)	110–120	116.07
Standard deviation (N)	26–31	27.38
Max. statistic value (N)	190–210	198.208
Min. statistic value (N)	20–40	33.91
Max. real value (N)	175–210	177.57
Min. real value (N)	50–70	60.05
Max. uplift at support 1 (mm)	48–55	53.4
Max. uplift at support 2 (mm)	48–55	51.9
Max. uplift at support 3 (mm)	48–55	53.8
Percentage of the loss of contact	0%	0%

catenary (see Fig. 1). The mesh has been obtained according to the methodology explained in Ref. [16], to which initial configuration has been arrived at from the mathematical formulation developed in Ref. [17]. Thus, only once the initial equilibrium problem is solved and the internal forces are computed, the finite element mesh is directly put on, avoiding, just like that, the iterative methodologies uniquely based on finite element formulations.

In order to reach an accurate performance of the cable system, the contact and messenger wires, a co-rotational beam formulation has been carried out, while a co-rotational truss formulation has been used for the droppers. Moreover, as these elements are not capable of resisting compression stress, the possible slackening of the droppers has been also taken into account. Both co-rotational formulations are based on the formulation developed by Crisfield in Refs. [18] and [19]. The commercial catenary used in the simulations that are presented in this paper is the catenary called Re250, which is employed in the Madrid-Sevilla high-speed service and whose geometric and mechanical characteristics can be found in the survey developed by Kiessling et al. in Ref. [20].

The pantograph model, on the contrary, has been carried out with a simple lumped-mass system with three degrees of freedom, as is usual in this kind of simulation, since its accuracy is generally enough without excessive computational costs. In addition, the pantograph has been preloaded with a constant force of 120 N.

The three-degrees-of-freedom pantograph depicted in Fig. 2 has been simulated with the mass, damp, and stiffness values collected in Table 1, which belong to the DSA-380E pantograph. Finally, the contact between the pantograph and the contact wire has been modeled using a penalty method, due to the simplicity of its implementation. Once again, this contact formulation has been established in the co-rotational framework developed in Ref. [19].

2.1 Catenary-Pantograph Interaction Validation. The dynamic performance of the catenary-pantograph system has been validated in accordance with the European Standard EN 50 318 (see Ref. [21]). This standard establishes the requirements for the validation of a catenary-pantograph interaction computational model. Essentially, this norm settles down a benchmark theoretical catenary-pantograph system and the range of results that must be accurately predicted by a simulation code. Tables 2 and 3 show a comparison of the obtained values over the reference model previously described and those required by the aforementioned standard. In addition, this norm also requires differences lower than 20% between the simulation results and two different experimental data series. The results of both comparisons can be seen in Table 4. Each of these experimental data belong to the pantograph DSA-380EU running at 300 km/h along the EAC-350 catenary (the catenary used along the Madrid-Barcelona high-speed line) and running at 280 km/h along the Re250 catenary (the catenary used along the Madrid-Sevilla high-speed line). As it can be seen, the values of the simulations are into the range established within the European Standard; thus, the performance of the model is satisfactory to carry out simulations of the catenary-pantograph dynamic interaction accurately enough.

3 Vehicle-Track Model

3.1 Vehicle Model. The vehicle model has been developed with a ten-degrees-of-freedom lumped-mass system linked by beam elements, as it is shown in the diagram of Fig. 3. This sort of model behaves more accurately than the simpler ones of three-degrees-of-freedom without excessive added computational cost. Moreover, its modular nature allows fitting of the lower part of the pantograph and the upper part of the vehicle by means of imposing that both displacements are equal.

Their stiffness and inertia values have been taken as equivalent to the simulated vehicles. Thus, in the simulations carried out, the values collected in Table 5, which belong to the 103 series of Alta Velocidad Española (AVE) trains taken from Refs. [22] and [23], have been used.

3.2 Track Model. The track model has been implemented as a classical beam over an elastic foundation. Its stiffness gathers the most important features of the track. This makes it possible to

Table 3 Validation of the catenary-pantograph model at 300 km/h

Magnitude	Range	Model
Mean contact force (N)	110–120	115.35
Standard deviation (N)	32–40	33.64
Max. statistic value (N)	210–230	216.27
Min. statistic value (N)	−5–20	14.44
Max. real value (N)	190–225	210.35
Min. real value (N)	30–55	40.87
Max. uplift at support 1 (mm)	55–65	62.7
Max. uplift at support 2 (mm)	55–65	63.1
Max. uplift at support 3 (mm)	55–65	62.0
Percentage of the loss of contact	0%	0%

Table 4 Comparison between experimental measurements and simulations in Re250 and EAC350 catenaries

	Catenary	Measurement	Simulation	Difference (%)
Standard deviation of contact force (N)	Re250	20.2	23.1	14.4
	EAC350	19.37	21.7	12
Max. uplift at support (mm)	Re250	95	88	−7.4
	EAC350	80	68	−15.4
Max. uplift of contact point (mm)	Re250	30	32	6.6
	EAC350	31	28	−7.4

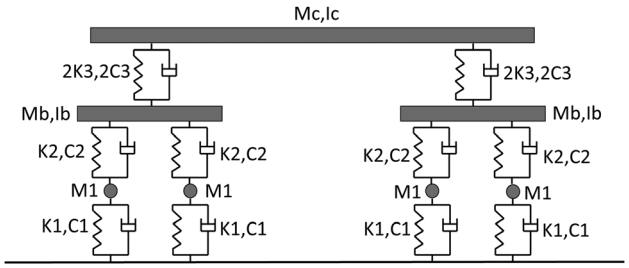

Fig. 3 Ten degrees of freedom vehicle model

Table 5 Simulation values of the 103 series of AVE

	1	2	3
M (kg)	350	0	0
C (Ns/m)	6.7×10^5	0	0.4
K (N/m)	8×10^9	0.3×10^6	4.4×10^6
mb (kg)		5.84×10^4	
Ib [m^4]		10^{-3}	
mc (kg)		6.19×10^4	
Ic (m^4)		10^{-3}	

simulate changes of the subsoil conditions, either by varying the stiffness of the springs or by adding surface defects on the rails by modifying the geometric position of the beams. The stiffness of the foundation is the result of adding the stiffness of the different parts or the track: pad, sleeper, ballast, sub-ballast, and surface of subgrade. The real measured values of the Madrid-Barcelona high-speed service, collected in Table 6 and provided in Ref. [22], have been considered in the simulations that are presented in this paper. Finally, the rail has been modeled using a Bernouilli beam approach with the characteristics presented in Table 6 too.

The study about French tracks carried out by Fryba, presented in Ref. [24], shows that irregularities of a track can be considered as a random variable, whose power spectral density function depends on the quality of the track. So the different types of tracks are split

Table 6 Properties of the rail and the track

Rail values	
E (GPa)	210
I (cm^4)	3313
ρ (kg/m^3)	7800
Rail road	
K (MN/m)	15.5
Distance between sleepers (m)	0.6

Table 7 Values for the random irregularities simulation

Class	1	2	3	4	5	6
A (mm)	15.53	8.85	4.92	2.75	1.57	0.98
ω_1			23.3			
ω_2			13.1			

up from the lowest (1) to the highest (6) quality class, which characterizes this random variable. It is also possible to include variations on the theoretical position of the track by the generation of a spatial series, whose power spectral density is given by Eq. (1),

$$\mathrm{PSD}_{\mathrm{irr}}(\omega_j) = \frac{A\omega_2^2\left(\omega_j^2 + \omega_1^2\right)}{\omega_j^4\left(\omega_j^2 + \omega_2^2\right)} \tag{1}$$

where the parameters A, ω_1, and ω_2 depend on the quality of the track (see Table 7). Thus, once the theoretical random positions are generated, it is possible to consider the position of the track from a more realistic point of view.

To know the power spectral density function allows us to generate a random profile of the track compatible with this spectra.

3.3 Vehicle-Track Interaction Validation. The contact between the wheels of the vehicle and the rail has been modeled, once again, using a segment-point penalty approach. In this sense, this contact is modeled from a macroscopic or numeric point of view without taking into account, for instance, gliding or local deformations of the contact surface. The set vehicle-track model has been validated by means of a reference simulation and the comparison of the obtained results against the values published by Koh et al. and gathered in Ref. [8]. Figure 4 reflects this comparison of the displacements of the track that have been calculated using the model that is presented in this paper and the values obtained from the previously mentioned reference. Owing to the fact that the simulation conditions and the conditions collected in Ref. [8] are not exactly the same, some differences are found. For example, the simulation has been carried out at a constant speed, while the results published in Ref. [8] presumably consider an acceleration, although this is not detailed in the paper. However, the general tendency of the results evidence that they are more than reasonable. In order to grow in confidence, the results obtained with the vehicle-track simulations have been also compared with the experimental values of the high-speed line Madrid-Barcelona presented by Melis [22]. Figure 5 shows the simulation values together with the experimental measurements. As the differences between both kind of values are also small, the results obtained with this validation and with the previous one are enough to assure that the interaction vehicle-track model exhibits a good performance.

4 Catenary-Pantograph-Vehicle-Track Model

The catenary-pantograph and the vehicle-track models previously presented have been joined up with each other in only one model by means of the well-known Lagrange multipliers. The dynamic simulation has been done applying the well-known Hilber-Hughes-

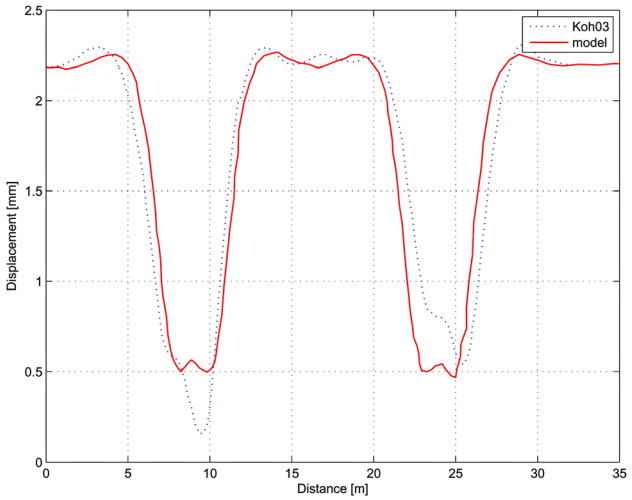

Fig. 4 Vehicle track interaction model validation

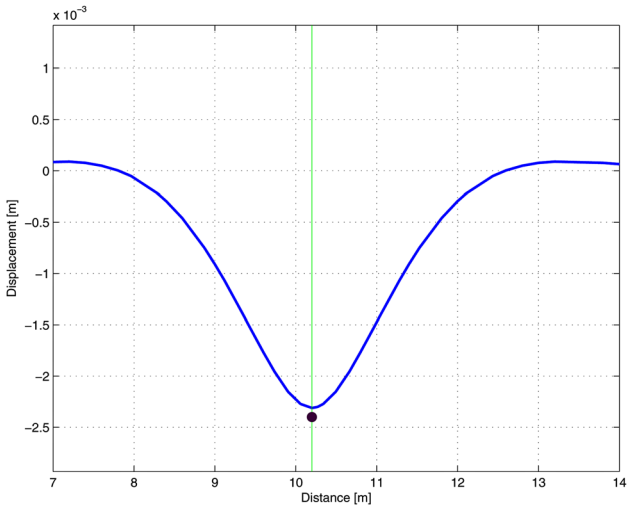

Fig. 5 Vehicle track interaction model validation comparison with experimental measurements

Taylor (HHT) time integration scheme, developed by Hilber et al. in Ref. [25], with a time step of 0.0025 s. This time integration method provides a good convergence and precision for this kind of nonlinear problem, which is essential for the different dynamic interactions and particularly the catenary-pantograph contact.

5 Simulations and Results

Both the simulations of the catenary-pantograph set, without considering the vehicle-track set, and the simulations taking into account this set and the existence of the vehicle and track have been done. The results obtained in both cases are exactly the same. However, in case of considering random irregularities in the track, the simulations show some differences. Due to the random nature of the irregularities and in order to have enough variability in the results, 30 different simulations of each irregularity degree have been carried out. These 30 simulations provide a wide range of variability in the track profile to analyze the results, assuming a normal distribution according to the limit central theorem.

The following graphs show the analysis of the obtained results by means of several box and whisker plots, which give information related to different relevant outcomes of the interaction: the range (understood as peak-to-peak amplitude) and the standard deviation of displacement and the maximum, minimum, and standard deviation of the contact force. The value that would correspond to these different parameters, in case track irregularities were not considered, is pointed out by means of a horizontal long line over the respective simulation. Although the differences are not relevant in absolute magnitude, it is noticeable that there exists an influence of the track profile in the amplitude of the pantograph displacements and contact forces. This influence is especially significant in the case of a worst quality track, where the relative difference between the displacement range in this worst case and the ideal track is over 60%, while this difference is reduced up to 5.7% in the case of considering the best quality of the track (see Fig. 6). Take notice that these percentages do not take into account outliers.

Moreover, the mean value of the displacements range is mostly higher than the mean value obtained without irregularities. Related to the tendencies of both displacements results, range and standard deviation, they present similar patterns, although data present higher dispersion in the last one, as it is shown in Figs. 6 and 7, respectively.

Speaking about the contact force, the differences are lower. The maximum contact force presents differences from 2:5 % to 0:6 % (see Fig. 8), while, in general terms, this is lower than the maximum contact force when the track irregularities are neglected. The minimum contact force, Fig. 9, shows differences from 7% for irregularity class 1 to 2.1% for the best one, while the mean value is approximately the same as the value obtained in the simulations without irregularities. Finally, the standard deviation of the contact force, Fig. 10, seems irrelevant, although it is for sure higher than that obtained without considering irregularities.

The previous results show the influence of the track profile within the amplitude of the displacements and, in a lower sense, within the contact force. Another way to prove the possible relations between the track profile and the catenary-pantograph interaction is considering these as a stochastic process. In Fig. 11, the autocorrelation function of the contact point displacement with and without considering the irregularities of the track is presented. In Fig. 12, the comparison explained just before is shown, though this is focused on the contact force.

According to these results, the frequency contain of the displacement of the contact point is mainly governed by the span length (the length of the span of the Re250 catenary is 65 m) and the inclusion of the irregularities of the track reduces the correlation of the displacements a little. Inclusion of track irregularities slightly drops the autocorrelation values at 65 and 130 m.

As it is shown, there is no correlation in the frequency contain of both signals. The influence of the track profile in the contact force is even less marked than the displacement ones. In this case,

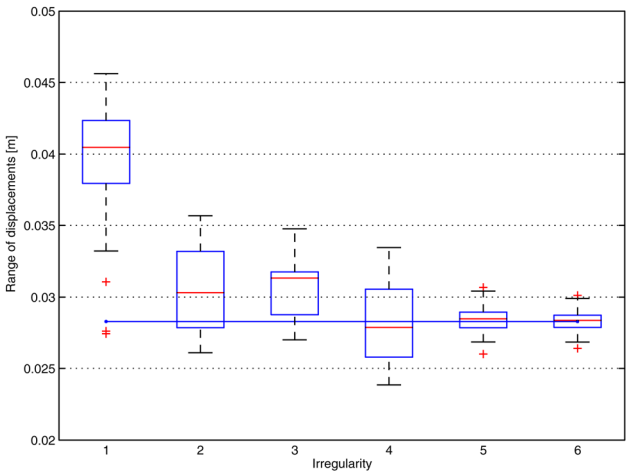

Fig. 6 Range of displacements

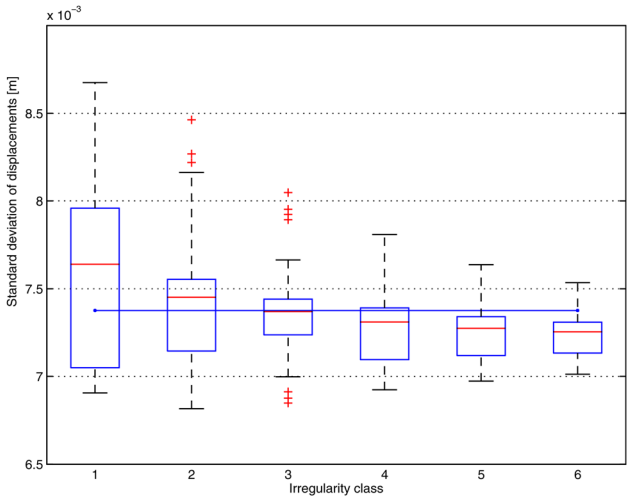

Fig. 7 Standard deviation of displacements

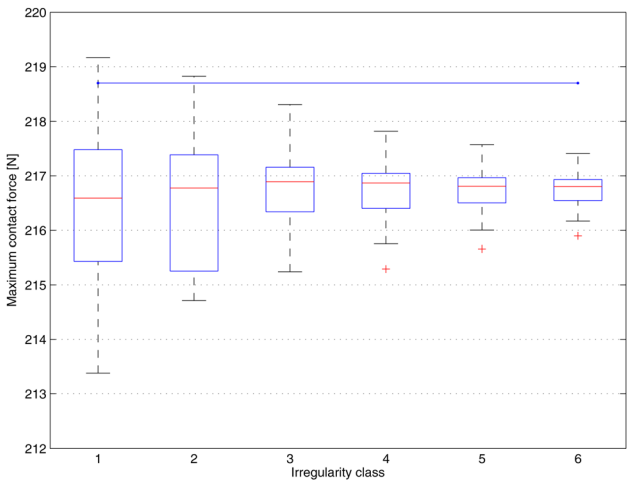

Fig. 8 Maximum contact force

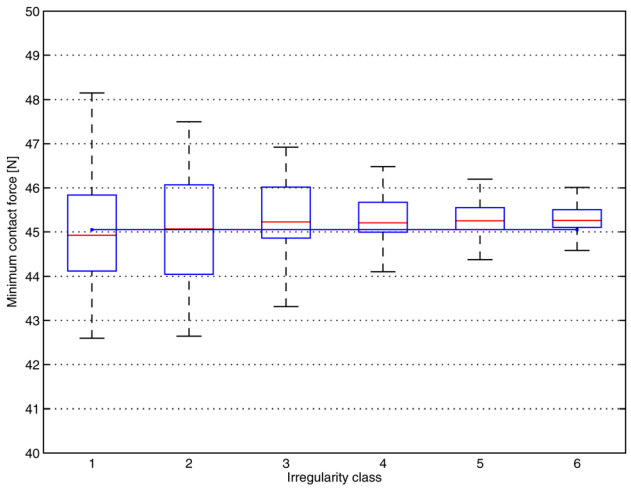

Fig. 9 Minimum contact force

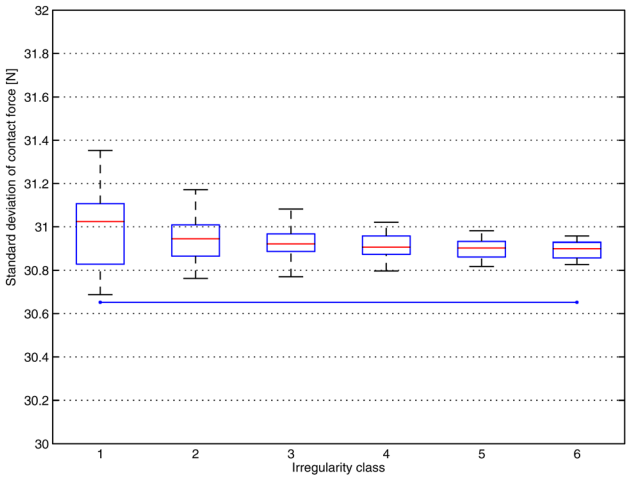

Fig. 10 Standard deviation of contact force

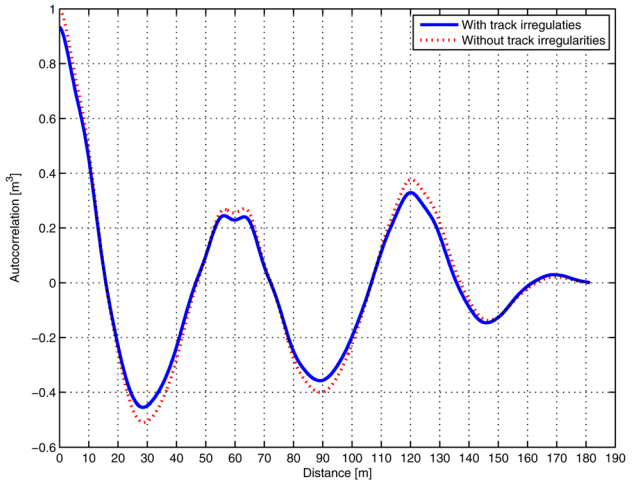

Fig. 11 Autocorrelation function of the displacements at the contact point

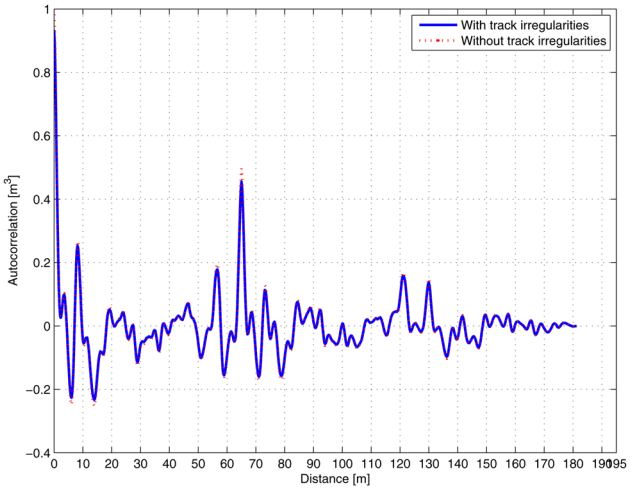

Fig. 12 Autocorrelation function of the contact force

Fig. 12 indicates that the contact forces are mainly governed by the length of the span and the distance between the droppers. Once again, the inclusion of track irregularities slightly drops the autocorrelation function at 65 m.

Figures 13 and 14 depict the coherence functions of the track profile with the contact point displacement for the first one and with the catenary-pantograph contact force for the second one. It is clear that the maximum coherence values are lower than 0.7;

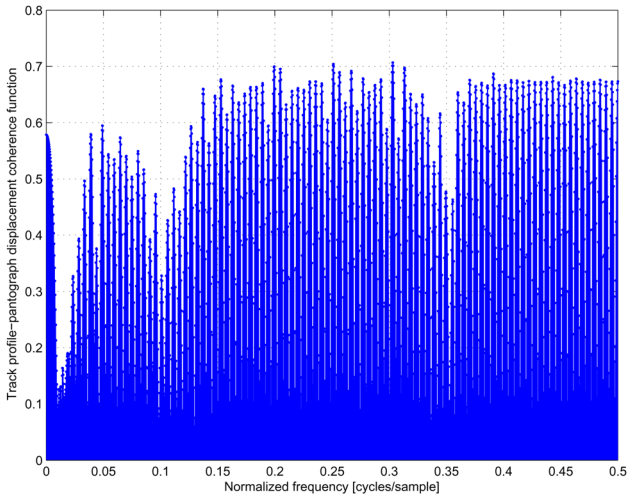

Fig. 13 Coherence function of the track profile and contact point displacement

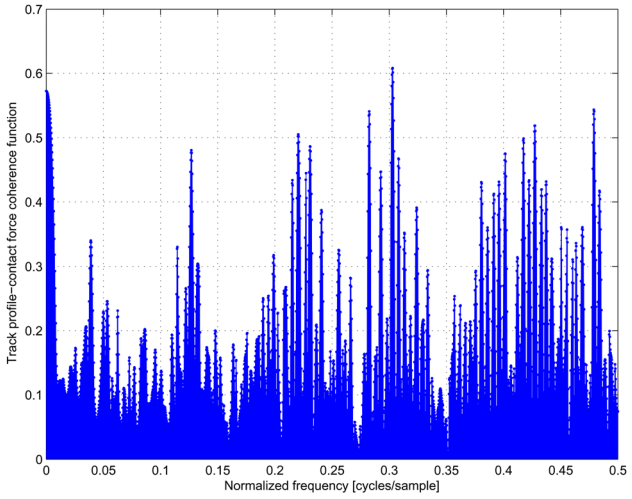

Fig. 14 Coherence function of the track profile and catenary-pantograph contact force

therefore, the influence between the track profile and the above-mentioned catenary values is poor.

6 Conclusions

Regarding the results presented in the previous sections, it is possible to conclude that the influence of the vehicle-track system on the catenary-pantograph interaction is not relevant. In fact, it has been proven that the track irregularities only introduce little differences in the contact force of the catenary-pantograph interaction, these differences being around 5%. However, in case of considering the displacement of the contact point, these differences could be much higher (over 60% in the case of lower quality track). This point could be important, because the European Standard EN 50 318 requires the comparison of the simulation results of the catenary-pantograph dynamic interaction with experimental results. The numerical results are not affected by the track, because most of the models of catenary-pantograph interaction do not take into account the vehicle dynamics and the track profile. In case of making these comparisons in low quality railways, the influence of the track and the vehicle within the experimental results could invalidate the numerical simulations. Despite certain of these conclusions have been already pointed out by other authors, the huge quantity of simulations carried out in this work reinforces their validity.

Acknowledgment

This work has been partially funded by the Spanish Ministerio de Ciencia e Innovacion under the project *Simulation of the wind effect in the interaction of catenary-pantographs of high speed train*, TRAN2009-13912-C-02-02/TREN. This support is gratefully acknowledged.

References

[1] Poetsch, G., Evans, J., Meisinger, R., Baldauf, W., Veitl, A., and Wallaschek, J., 1997, "Pantograph/Catenary Dynamics and Control," Veh. Syst. Dyn., **28**, pp. 159–195.
[2] Shabana, A., and San, J., 2001, "A Survey of Rail Vehicle Track Simulations and Flexible Multibody Dynamics," Nonlinear Dyn., **26**, pp. 179–210.
[3] Collina, A., and Bruni, S., 2002, "Numerical Simulation of Pantograph-Overhead Equipment Interaction," Veh. Syst. Dyn., **38**(4), pp. 261–291.
[4] Wu, T., and Brennan, M., 1999, "Dynamic Stiffness of a Railway Overhead Wire System and Its Effect on Pantographcatenary System Dynamics," J. Sound Vib., **219**(3), pp. 483–502.
[5] Lopez-Garcia, O., Carnicero, A., and Marono, J., 2007, "Influence of Stiffness and Contact Modelling on Catenary Pantograph System Dynamics," J. Sound Vib., **299**, pp. 806–821.
[6] Arnold, M., and Simeon, B., 2000, "Pantograph and Catenary Dynamics: A Benchmark Problem and Its Numerical Solution," Appl. Numer. Math., **34**(4), pp. 345–362.
[7] Olsson, M., 1985, "Finite Element, Modal Co-ordinate Analysis of Structures Subjected to Moving Loads," J. Sound Vib., **99**, pp. 1–12.
[8] Koh, C., Ong, J., Chua, D., and Feng, J., 2003, "Moving Element Method for Train-Track Dynamics," Int. J. Numer. Methods Eng., **56**, pp. 1549–1567.
[9] Lou, P., and Zeng, Q., 2005, "Formulation of Equations of Motion of Finite Element Form for Vehicle-Track-Bridge Interaction System With Two Types of Vehicle Model," Int. J. Numer. Methods Eng., **62**, pp. 435–474.
[10] Lou, P., 2005, "Vertical Dynamic Responses of a Simply Supported Bridge Subjected to a Moving Train With Two-Wheel Set Vehicles Using Modal Analysis Method," Int. J. Numer. Methods Eng., **64**, pp. 1207–1235.
[11] Zhai, W., Wang, K., and Cai, C., 2009, "Fundamentals of Vehicle-Track Coupled Dynamics," Veh. Syst. Dyn., **47**(11), pp. 1349–1376.
[12] Pombo, J., Ambrosio, J., and Silva, M., 2007, "A New Wheel-Rail Contact Model for Railway Dynamics," Veh. Syst. Dyn., **45**.
[13] Pombo, J., Ambrosio, J., Pereira, M., Verardi, R., Ariaudo, C., and Kuka, N., 2011, "Influence of Track Conditions and Wheel Wear State on the Loads Imposed on the Infrastructure by Railway Vehicles," Comput. Struct., **89**, pp. 1882–1894.
[14] Seo, J., Sugiyama, H., and Shabana, A., 2005, "Three-Dimensional Large Deformation Analysis of the Multibody Pantograph/Catenary Systems," Nonlinear Dyn., **42**, pp. 199–215.
[15] Zhai, W., and Cai, C., 1998, "Effect of Locomotive Vibration on Pantograph-Catenary System Dynamics," Veh. Syst. Dyn. Suppl., **28**, pp. 47–58.
[16] Carnicero, A., Lopez-Garcia, O., Torres, V., and Jimenez-Octavio, J., 2006, "An Algorithm Based on Finite Element Method and Catenary Equation to Compute the Initial Equilibrium of Railway Overhead," Eighth International Conference on Computational Structures Technology, Las Palmas de Gran Canaria (España), Sept. 12-15.
[17] Such, M., Jimenez-Octavio, J., Carnicero, A., and Lopez-Garcia, O., 2009, "An Approach Based on the Catenary Equation to Deal With Static Analysis of Three Dimensional Cable Structures," Eng. Struct., **31**, pp. 2162–2170.
[18] Crisfield, M., 1997. *Non-linear Finite Element Analysis of Solids and Structures*, Vol. 1, Wiley, New York.
[19] Crisfield, M., 1997, *Non-linear Finite Element Analysis of Solids and Structures*, Vol. 2, Wiley, New York.
[20] Kiessling, F., Puschmann, R., Schmieder, A., and Schneider, E., 2009, *Contact Lines for Electric Railways*. Publicis Publishing, Erlangen.
[21] CENELEC, 2002. *EN50318:2002, Railway Applications. Current Collection Systems. Validation of Simulation of the Dynamic Interaction Between Pantograph and Overhead Contact Line*, July ed. European Committee for Electrotechnical Standardization, Brussels.
[22] Melis, M., 2008, *Dinamica Vertical de la Via, Catedra de Ferrocarriles (in Spanish)*, ETSICCyP, Madrid.
[23] Gabaldon, F., Riquelme, F., Goicolea, J., and Arribas, J., 2005, Dynamic Analysis of Structures Under High Speed Train Loads: Case Studies in Spain. Dynamics of High-Speed Railway Bridges, Advanced Course, Porto, Faculty of Engineering, University of Porto, London.
[24] Frýba, L., 1996, *Dynamics of Railway Bridges*, Thomas Telford.
[25] Hilber, H. M., Hughes, T. R., and Talor, R. L., 1977, "Improved Numerical Dissipation for Time Integration Algorithms in Structural Dynamics," Earthquake Eng. Struct. Dyn., **5**, pp. 282–292.